PCP
PLANT & CELL PHYSIOLOGY

Cuticular Wax Biosynthesis is Up-Regulated by the MYB94 Transcription Factor in Arabidopsis

Saet Buyl Lee and Mi Chung Suh*

Department of Bioenergy Science and Technology, Chonnam National University, Gwangju, 500-757, Korea
*Corresponding author: E-mail, mcsuh@chonnam.ac.kr; Fax, +82-62-530-2047.
(Received August 28, 2014; Accepted October 5, 2014)

Regular Paper

The aerial parts of all land plants are covered with hydrophobic cuticular wax layers that act as the first barrier against the environment. The *MYB94* transcription factor gene is expressed in abundance in aerial organs and shows a higher expression in the stem epidermis than within the stem. When seedlings were subjected to various treatments, the expression of the *MYB94* transcription factor gene was observed to increase approximately 9-fold under drought, 8-fold for ABA treatment and 4-fold for separate NaCl and mannitol treatments. MYB94 harbors the transcriptional activation domain at its C-terminus, and fluorescent signals from MYB94:enhanced yellow fluorescent protein (eYFP) were observed in the nucleus of tobacco epidermis and in transgenic Arabidopsis roots. The total wax loads increased by approximately 2-fold in the leaves of the *MYB94*-overexpressing (*MYB94* OX) lines, as compared with those of the wild type (WT). MYB94 activates the expression of *WSD1*, *KCS2/DAISY*, *CER2*, *FAR3* and *ECR* genes by binding directly to their gene promoters. An increase in the accumulation of cuticular wax was observed to reduce the rate of cuticular transpiration in the leaves of *MYB94* OX lines, under drought stress conditions. Taken together, a R2R3-type MYB94 transcription factor activates Arabidopsis cuticular wax biosynthesis and might be important in plant response to environmental stress, including drought.

Keywords: Arabidopsis • Cuticular wax • MYB94 • R2R3-type MYB transcription factor • Transcriptional regulation.

Abbreviations: CaMV, *Cauliflower mosaic virus*; DAPI, 4′,6-diamidino-2-phenylindole; ECR, enoyl-CoA reductase; EMSA, electrophoretic mobility shift assay; ER, endoplasmic reticulum; eYFP, enhanced yellow fluoresent protein; FAE, fatty acid elongase complex; FAR3/CER4, fatty acyl-CoA reductase; GUS, β-glucuronidase; HCD, β-hydroxyacyl-CoA dehydratase; HDG1, homeodomain glabrous1; KCR, β-ketoacyl-CoA reductase; KCS, β-ketoacyl-CoA synthase; LACS, long chain acyl-CoA synthetase; LTPG, glycosylphosphatidylinositol-anchored lipid transfer protein; MAH1, midchain alkane hydroxylase1; MBP, maltose-binding protein; MS, Murashige and Skoog; NLS, nuclear localization signal; OX, overexpressing; TF, transcription factor; qRT–PCR, quantitative real-time reverse transcription–PCR; VLCFA, very-long-chain fatty acid; WIN1/SHN1, wax inducer1/shine1; WSD1, bifunctional wax synthase/acyl-CoA:diacylglycerol acyltransferase; WT, wild type.

Introduction

The aerial part of plant surfaces is covered with a hydrophobic layer comprised of cutin polyesters and intra- and epicuticular waxes (reviewed by Bernard and Joubès 2013, Yeats and Rose 2013). The cuticle prevents non-stomatal water loss and gaseous exchange, scatters UV radiation, and repulses pathogen spores and atmospheric pollutants, such as acid rain, ozone and carbon dioxide (reviewed by Shephered and Griffiths 2006, Bernard and Joubès 2013). Cuticular waxes consist of solvent-soluble lipids, which are made of very-long-chain fatty acids (VLCFAs; >20 carbons in length) and their derivatives (including alkanes, aldehydes, ketones, primary and secondary alcohols and wax esters) with smaller amounts of triterpenoids and phenylpropanoids (Jetter et al. 2006). Insoluble cutin layers are known to have a polyester structure that contains glycerols esterified with C16 and C18 fatty acids and their derivatives, such as hydroxyl and dicarboxylic fatty acids, and phenylpropanoids, such as coumaric and ferulic acids (Kunst and Samuels 2009, Beisson et al. 2012).

Cuticular waxes are known to be synthesized in epidermal cells (Suh et al. 2005) where C16 and C18 fatty acids, which are synthesized de novo in the plastids, are further elongated into VLCFAs by an endoplasmic reticulum (ER)-localized fatty acid elongase complex (FAE). FAE consists of β-ketoacyl-CoA synthase (KCS), β-ketoacyl-CoA reductase (KCR), β-hydroxyacyl-CoA dehydratase (HCD) and enoyl-CoA reductase (ECR) (Kunst and Samuels 2009, Lee and Suh 2013, Li-Beisson et al. 2013). Recently CER2 and CER2-LIKE1/CER26, which have homology to BAHD acyltransferase, were reported to function in the synthesis of VLCFAs of >26 carbons in length (Haslam et al. 2012, Pascal et al. 2013). The synthesized VLCFAs are activated into VLCFA-CoAs by a long chain acyl-CoA synthetase (LACS) (Lu et al. 2009, Weng et al. 2010), and the VLCFA-CoAs are modified via the alkane-forming and alcohol-forming pathways (Kunst and Samuels 2009, Lee and Suh 2013, Li-Beisson et al. 2013). In the alkane-forming pathway, VLCFA-CoAs are catalyzed into alkanes by a CER1, CER3 and Cyt b_5 complex (Bernard et al. 2012), and the alkanes are oxidized into secondary

Plant Cell Physiol. 56(1): 48–60 (2015) doi:10.1093/pcp/pcu142, Advance Access publication on 11 October 2014, available online at www.pcp.oxfordjournals.org

alcohols and ketones by a midchain alkane hydroxylase1 (MAH1) (Greer et al. 2007). In the alcohol-forming pathway, VLCFA-CoAs are reduced into primary alcohols by a fatty acyl-CoA reductase (FAR3/CER4) (Rowland et al. 2006), and the primary alcohols are esterified with C16-CoAs by a bifunctional wax synthase/acyl-CoA:diacylglycerol acyltransferase (WSD1) (Li et al. 2008). The wax precursors synthesized in the ER are exported to the extracellular space via both homodimers (ABCG11/WBC11) and heterodimers (ABCG11/WBC11 and ABCG12/CER5) of ATP-binding cassette (ABC) transporters (McFarlane et al. 2010). Glycosylphosphatidylinositol (GPI)-anchored LTPs (LTPGs), which are attached to the outer surface of the plasma membrane via a GPI anchor, were reported to be directly or indirectly involved in wax export (DeBono et al. 2009, Lee et al. 2009a, Kim et al. 2012). Wax transport from the ER to the plasma membrane was recently reported to require Golgi- and *trans*-Golgi network-mediated vesicle trafficking (McFarlane et al. 2014).

To date, there are pieces of several evidence indicating that cuticular wax biosynthesis is regulated at the transcriptional level (Bernard and Joubès 2013, Li-Beisson et al. 2013). Arabidopsis WAX INDUCER1/SHINE1 (WIN1/SHN1) encoding an AP2/EREBP-type transcription factor (TF) activates cuticular wax and cutin biosynthesis by inducing the expression of *CER1*, *KCS1*, *CER2*, *LACS2*, *GPAT4*, *CYP86A4*, *CYP86A7* and *HTH*-like genes, and the total amount of cuticular wax and cutin increases in transgenic Arabidopsis that overexpresses WIN1 (Broun et al. 2004, Kannangara et al. 2007). It was reported later that WIN1/SHN1 regulates cutin biosynthesis via direct binding to the promoter of the *LACS2* gene (Kannangara et al. 2007). Oshima et al. (2013) have characterized the R2R3-type MYB16 and MYB106 TFs involved in cuticle development, and, in particular, MYB106 was identified to be a positive regulator of WIN1/SHN1 expression. In addition, MYB30, MYB41, CURLY FLAG LEAF1 (CFL1; containing WW domain protein) and HOMEODOMAIN GLABROUS1 (HDG1; classified in the Class IV HD-ZIP gene family) have been reported to function as positive regulators in cuticular wax biosynthesis or in cuticle deposition (Cominelli et al. 2008, Raffaele et al. 2008, Wu et al. 2011). In particular, MYB41 activates the synthesis and deposition of both aliphatic suberin-type polyesters and suberin-associated wax-type compounds in Arabidopsis and *Nicotiana benthamiana* (Kosma et al. 2014). An AP2/ERF type DEWAX TF was reported to repress cuticular wax biosynthesis via direct interaction with *FAR6*, *CER1*, *LACS2* and *ECR* gene promoters, and the total wax loads in Arabidopsis stems were regulated by the expression of a DEWAX TF that is diurnally regulated during light and dark cycles (Go et al. 2014). Under drought stress, the total amounts of cuticular wax increased by approximately 2-fold in Arabidopsis and in tree tobacco (Cameron et al. 2006, Kosma et al. 2009). Up-regulation of cuticular wax biosynthesis was known to be mediated by a drought- and ABA-inducible MYB96 TF (Seo et al. 2011). MYB96 enhances the expression of *KCS1*, *KCS2*, *KCS6* and *KCR1* genes that are involved in the biosynthesis of VLCFAs, which in turn are essential precursors for cuticular wax biosynthesis. Under drought, the total wax loads in wild-type (WT) and in *myb96-1* Arabidopsis leaves increased approximately 4- and 2-fold, respectively, suggesting that additional TFs might be present in drought-induced wax accumulation.

In the phylogenetic tree of the Arabidopsis R2R3-type MYB TFs, MYB94 is classified very close to MYB96. In this study, the MYB94 transcriptional activation domain was analyzed in a yeast-based transactivation assay. We visualized the subcellular localization of fluorescent MYB94:enhanced yellow fluorescent protein (eYFP) proteins in tobacco epidermis and in transgenic Arabidopsis roots, and we also observed the expression patterns of *MYB94* in various Arabidopsis organs and in seedlings after treatments with ABA, drought, salt and osmotic stress. Finally we observed how the overexpression of *MYB94* activates cuticular wax biosynthesis in Arabidopsis via up-regulated expression of *WSD1*, *KCS2/DAISY*, *CER2*, *FAR3* and *ECR* genes. These results suggest that MYB94 might be an additional TF in the activation of cuticular wax biosynthesis in Arabidopsis under drought stress.

Results

Isolation of the *MYB94* gene encoding the R2R3-type MYB transcription factor

In order to characterize the novel TF that is involved in the activation of cuticular wax biosynthesis under drought stress, 147 TFs that showed higher expression in stem epidermal cells than in stem cells were isolated based on an Arabidopsis stem epidermis microarray analysis (Suh et al. 2005). They were further screened according to the induced expression patterns after treatments with ABA and/or drought stress using the Arabidopsis microarray database (www.arabidopsis.org). Sixteen MYB TFs, including a MYB96 TF, were selected (**Supplementary Fig. S1A**). Finally we isolated the *MYB94* (At3g47600) gene that is up-regulated approximately 5-fold in stem epidermal cells relative to cells in the stems, and this was induced by approximately 10- and 2-fold in Arabidopsis seedlings after 10 μM ABA treatment and drought stress, respectively. In addition, *MYB96* was observed to be very closely located in the phylogenetic tree of 126 R2R3-type MYB TFs (**Supplementary Fig. S1B**).

MYB94 contains a transcriptional activation domain in its C-terminal region and the fluorescent MYB94:eYFP is localized to the nucleus.

A MYB94 protein harboring 333 amino acid residues contains R2 (amino acid residues 9–63) and R3 (amino acid residues 69–117) domains with the conserved amino acid motifs R2 [-W-(X_{19})-W-(X_{19})-W-] and R3 [-F-(X_{18})-W-(X_{18})-W-] that are known to be essential for DNA binding (**Fig. 1A**; Dubos et al. 2010). The transcriptional activation domain of the MYB94 protein was subsequently investigated via yeast-based transactivation assay (Park et al. 2009). The full-length (F; amino acid residues 1–333), N-terminal region (N; amino acid residues 1–123) and C-terminal region (C; amino acid residues 124–333)

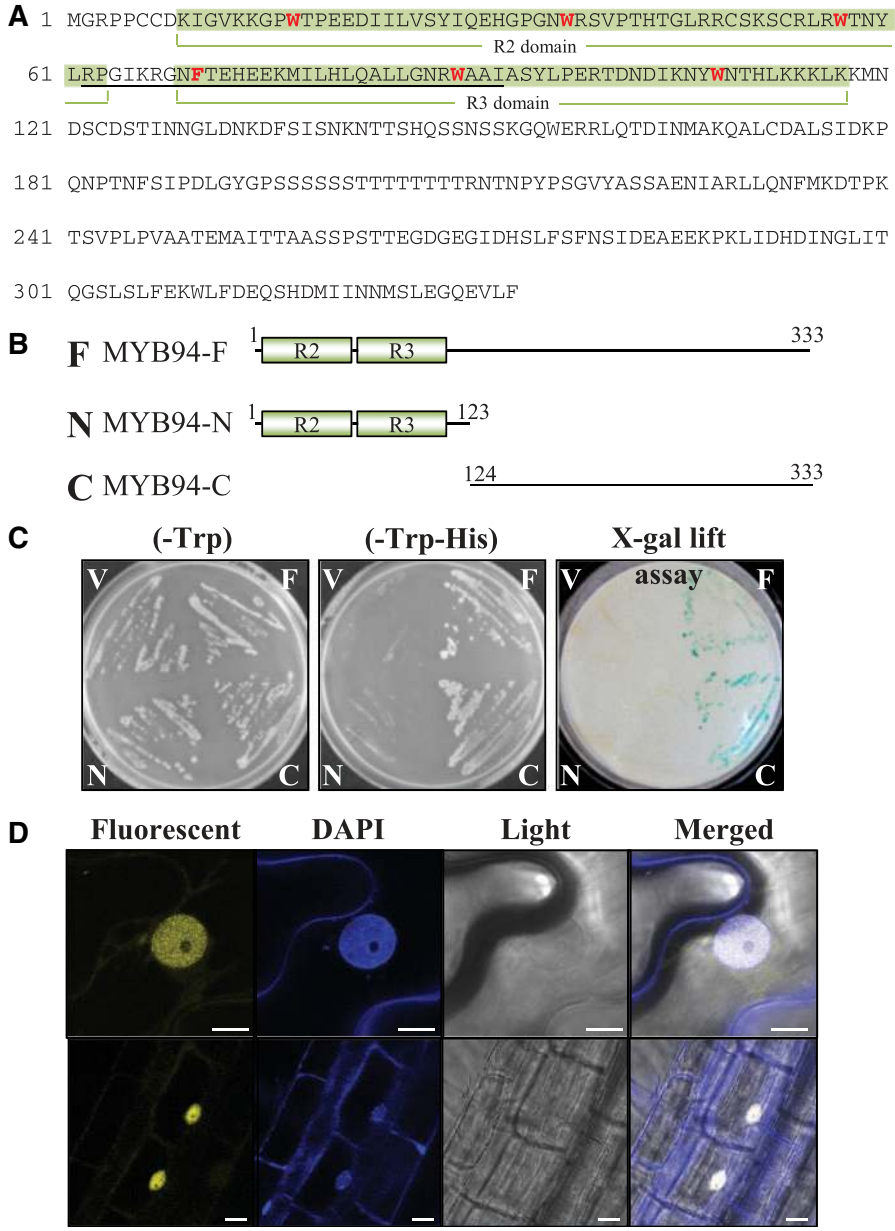

Fig. 1 MYB94 is a transcriptional activator localized in the nucleus. (A) Amino acid sequences of the MYB94 protein. The two green boxes denote the conserved R2 and R3 domains required for DNA binding. The highly conserved amino acid residues are shown in red, and the nuclear localization signal motif is underlined. (B) Schematic diagram for the full-length protein and deletion constructs of MYB94 in pGBKT7 vector. F, the full-length MYB94 protein in the pGBKT7 vector; N, the N-terminal region of MYB94 protein in the pGBKT7 vector; C, the C-terminal region of the MYB94 protein in the pGBKT7 vector. (C) Transactivation assay of MYB94 in yeast cells. The transformed yeast cells were grown on selective medium SD/−Trp (left) and SD/−Trp−His (middle) supplemented with 25 mM 3-amino-1,2,4-aminotriazole. An X-gal lift assay was carried out using an SD/−Trp−His plate (right). V, yeast transformed with the pGBKT7 vector; F, N and C, yeast transformed with the F, N and C constructs, respectively, as shown in (B). (D) Subcellular localization of the MYB94:eYFP in tobacco epidermis (upper) and a transgenic Arabidopsis root (lower). DAPI staining was performed to visualize the nucleus, and the images were acquired using a laser confocal scanning microscope with a YFP or a UV filter. Scale bars = 10 μm.

of MYB94 were translationally fused to the GAL4 DNA-binding domain in the pGBKT7 plasmids (Fig. 1B; Clontech). When the constructed plasmids were induced in the yeast Y190 strain containing the *GAL1* promoter and *HIS3* and *lacZ* reporter genes, β-galactosidase activity was observed in yeast cells harboring MYB94-F or MYB94-C plasmids, but not in yeast cells containing pGBKT7 (V) or MYB94-N plasmids (Fig. 1C). The results indicate that the C-terminal region of MYB94 functions as a transcriptional activation domain.

To investigate the intracellular location of MYB94 TF, a full-length (999 bp) MYB94 without the termination codon (TAG) was translationally fused to the 5′ end of eYFP. The generated construct was introduced into tobacco leaf epidermal cells via *Agrobacterium*-mediated infiltration (Sparkes et al. 2006) or

was transformed into Arabidopsis via floral dip (Zhang et al. 2006). The fluorescent signals from the MYB94:eYFP construct were observed in the nucleus of tobacco leaf epidermal cells and in 2-week-old transgenic Arabidopsis roots, and these merged with the fluorescent signals from 4′,6-diamidino-2-phenylindole (DAPI) staining (**Fig. 1D**), indicating that the fluorescent MYB94:eYFP was localized in the nucleus.

Spatial and temporal expression patterns of *MYB94* in various Arabidopsis organs and in seedlings after treatments with ABA, drought, salt and osmotic stress

To investigate the expression levels of the *MYB94* gene in various Arabidopsis organs and in seedlings after treatment with ABA and abiotic stresses, quantitative real-time reverse transcription–PCR (qRT–PCR) was performed. The *MYB94* transcripts were ubiquitously expressed in germinating seeds, rosette and cauline leaves, flower buds, open flowers, stems and developing siliques, but they were not or were very weakly observed in pollen and roots. In addition, the expression of the *MYB94* gene was approximately five times higher in stem epidermal peels than in the stems (**Fig. 2A**). The expression of the *MYB94* gene was also analyzed in 10-day-old Arabidopsis seedlings after treatment with drought stress, 100 μM ABA, 200 mM NaCl and 200 mM mannitol. When the expression of the *rd29A* gene was induced as a control of water-deficit response (Liu et al. 1998), the levels of *MYB94* transcripts increased by approximately 9-fold in response to drought, 8-fold in response to ABA and 4-fold for NaCl and mannitol treatments, separately (**Fig. 2B**).

β-Glucuronidase assay (GUS) was performed in transgenic Arabidopsis plants expressing the *GUS* gene under the control of the *MYB94* promoter (approximately 4.2 kb) to examine the spatial and temporal expression of the *MYB94* gene. More than 30 independent transgenic lines were screened for GUS activity, and the expression of the *GUS* gene was observed in the aerial part of a 7-day-old seedling, stem epidermis, stem cortex, phloem and xylem cells of stems, leaves including trichomes, sepals, anther and anther filaments, the upper portion of the stigma and the silique walls, but not in the root and the developing seeds (**Fig. 2Ca–g**).

The amounts of cuticular waxes increased in the leaves of transgenic Arabidopsis plants overexpressing *MYB94*

In order to investigate the function of the *MYB94* gene in planta, the Arabidopsis transgenic plants overexpressing *MYB94* (*MYB94* OX) were generated under the *Cauliflower mosaic virus* (CaMV) 35S promoter control (**Fig. 3A**). The *MYB94* transcript levels in the leaves of *MYB94* OX lines were elevated by approximately 15–500 times that of the WT (**Fig. 3B**). Although no significantly altered phenotype in the *MYB94* OX lines was observed during growth and development under long-day conditions (16 h/8 h; light/dark), as compared with the WT, scanning electron microscopy analysis showed that the deposition of epicuticuar wax crystals was detected on the leaves of *MYB94* OX lines, but was not observed on the leaves of the WT (**Fig. 3Ca–d**).

In addition, transgenic Arabidopsis plants expressing the *MYB94* gene under the control of the β-estradiol-inducible promoter were generated and, after treatment with β-estradiol, epicuticular wax crystals formed on the leaves of transgenic Arabidopsis expressing *MYB94* but not on the leaves of WT or mock-treated leaves of transgenic Arabidopsis expressing *MYB94* (**Fig. 3D**).

The amount and the composition of cuticular waxes were subsequently measured from leaves and stems of *MYB94* OX lines and from WT plants using gas chromatography (GC). The total wax loads increased by approximately 1.7- and 1.3-fold in the leaves of the *MYB94* OX-1 line and the OX-5 line, respectively, but was not significantly altered in the leaves of *MYB94* OX-3 relative to the WT (**Fig. 4A**), suggesting that an increase in the total wax loads is correlated with the up-regulated expression of the *MYB94* gene. In addition, the levels of C28 and C30 VLCFAs, C28, C30 and C32 aldehydes, and C29, C31, C33 alkanes synthesized by the alkane-forming pathway and the amounts of C26, C28, C30 and C32 primary alcohols produced by the alcohol-forming pathway were significantly increased in *MYB94* OX-1 and in OX-5 lines compared with the WT (**Fig. 4B**). However, no significant increase in the total wax loads was observed in the stems of *MYB94* OX-1 and OX-5 lines compared with those of the WT (**Supplementary Fig. S2**).

To examine if overexpression of *MYB94* affects cutin biosynthesis, the amounts and composition of cutin monomers were measured in the leaves of *MYB94* OX-1 and WT plants using GC–mass spectrometry (GC/MS). The total amounts of cutin monomers increased by approximately 18% in *MYB94* OX-1 relative to the WT (**Supplementary Fig. S3A**). In particular, the amounts of hydroxy fatty acids, including C18:1 and C18:2 ω-hydroxy fatty acids, and dicarboxylic fatty acids, including C18:2 dicarboxylic fatty acids, increased by 39% and 24% in *MYB94* OX-1 relative to the WT (**Supplementary Fig. S3B**).

The expression of genes involved in cuticular wax biosynthesis was up-regulated in leaves of transgenic Arabidopsis plants overexpressing *MYB94*

To investigate the target genes of the MYB94 TF, total RNAs were extracted from the leaves of the WT and the *MYB94* OX-1 lines under the control of the CaMV 35S promoter and were subjected to a microarray analysis using the Arabidopsis Affymetrix ATH1 GeneChip, which contains >22,500 probe sets. About 230 genes were up-regulated by approximately 1.5-fold in *MYB94* OX-1 relative to the WT. The list of genes that were up-regulated by >1.5-fold in *MYB94* OX-1 relative to the WT, and that are involved in cuticular wax biosynthesis, is shown in **Fig. 5A**. Interestingly, the expression of genes involved in cutin synthesis was not significantly up-regulated in *MYB94* OX-1 as compared with the WT (**Supplementary Table S1**). qRT-PCR analysis showed that the *MYB94*, *WSD1*, *KCS2/DAISY*, *CER1*, *CER2*, *FAR3* and *ECR* transcript levels were up-regulated by approximately 2.5- to 30-fold, but no significant changes in

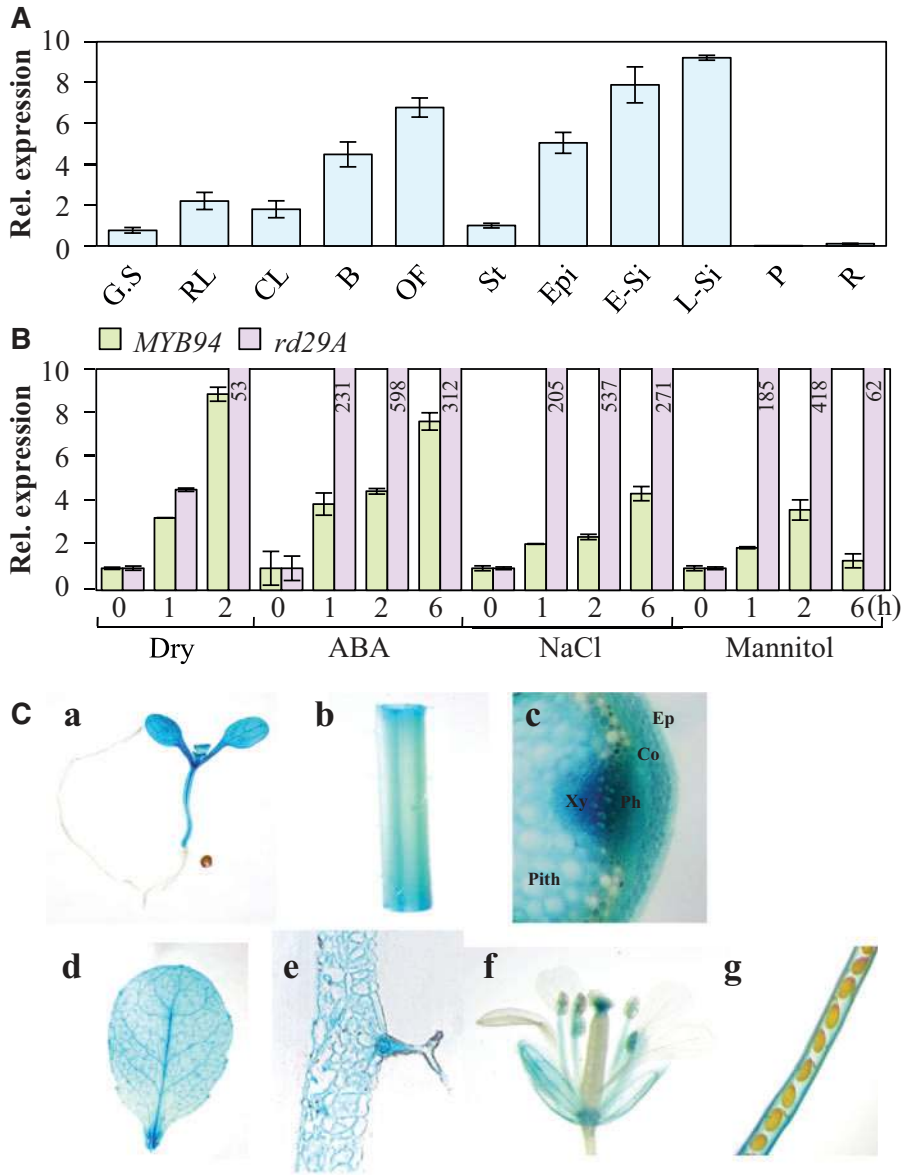

Fig. 2 Expression of *MYB94* in Arabidopsis. (A) qRT-PCR analysis of *MYB94* in various Arabidopsis organs or tissues. Total RNA was isolated from 1-day-old germinating seeds (G.S), rosette leaves (RL), cauline leaves (CL), flower buds (B), open flowers (OF), stems (St), stem epidermis (Epi), developing siliques at stages 3–5 (E-Si; Winter et al. 2007), developing siliques at stages 6–8 (L-Si), pollen (P) and roots (R) of 6-week-old plants. (B) Expression of *MYB94* transcripts by exogenous application of ABA and treatments with drought, salt and osmotic stresses. Total RNA was isolated from 10-day-old Arabidopsis seedlings, which were incubated in liquid MS medium supplemented with 200 mM NaCl, 200 mM mannitol or 100 μM ABA for 1, 2 and 6 h. For drought stress treatment, the seedlings were transferred to filter papers and were air-dried for 1 and 2 h. The isolated RNA was subjected to qRT–PCR. The *PP2A* (At1g13320) gene was used to determine the quantity and quality of the cDNAs, and *rd29A* (At5g52310) was used as a drought stress-inducible marker. Each value is the mean of triplicate experiments. (C) GUS expression under the control of the *MYB94* promoter in transgenic Arabidopsis plants. The *MYB94* promoter::GUS construct was transformed into Arabidopsis plants, and independent transgenic lines were stained with 1 mM 5-bromo-4-chloro-3-indolyl-β-D-glucuronide. (a) Seven-day-old seedling; (b) stem; (c) cross-section of stem; (d) leaf; (e) cross-section of leaf (f) flower (g) silique. Ep, epidermis; Co, cortex; Ph, phloem; Xy, xylem.

the levels of *KCS1* transcripts were observed in *MYB94* OX-1 relative to the WT (**Fig. 5B**).

In addition, significant up-regulation of *MYB94*, *WSD1*, *KCS2/DAISY*, *CER1*, *CER2*, *FAR3* and *ECR* genes was observed in the leaves of transgenic Arabidopsis expressing *MYB94* under the control of the β-estradiol promoter, but not in the WT, at 2, 6, 12 and 24 h after treatment with 10 μM β-estradiol. However, the expression of those genes was not significantly altered in either mock-treated WT or transgenic leaves (**Fig. 5C**). These results indicate that the MYB94 TF activates cuticular wax biosynthesis via up-regulation of genes involved in wax biosynthesis.

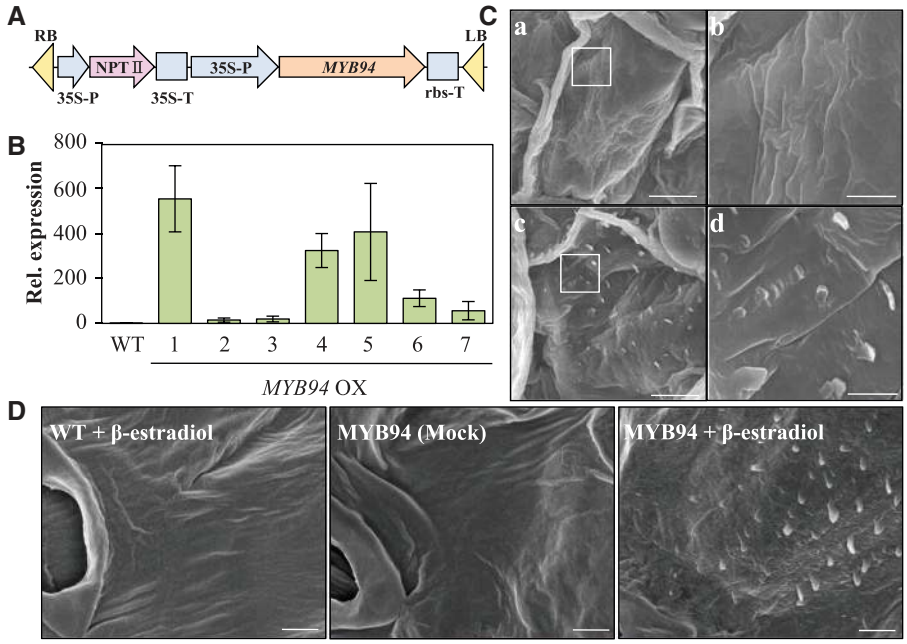

Fig. 3 Constitutive or β-estradiol-inducible expression of *MYB94* in transgenic Arabidopsis plants. (A) Schematic diagram of *MYB94* in the pPZP212 vector under the control of the CaMV 35S promoter. 35S-P, CaMV 35S promoter; 35S-T, CaMV 35S terminator; rbs-T, terminator of ribulose 1,5-biphosphate carboxylase/oxygenase small subunit; RB, T-DNA right border sequences; LB, T-DNA left border sequences.(B) The relative expression level of *MYB94* genes in the leaves of WT and *MYB94* overexpression (*MYB94* OX) lines. The total RNA was isolated from the leaves of WT and *MYB94* OX lines and was subjected to qRT–PCR. The *PP2A* (At1g13320) gene was used to determine the quantity and quality of the cDNAs. Each value is the mean of triplicate experiments. (C) Scanning electron microscopy (SEM) images of epicuticular wax crystals on the leaves. The rosette leaves of 3-week-old WT (a, b) and *MYB94* OX (c, d) plants grown in soil were used to perform a SEM analysis. (b, d) White boxes in (a) and (c) are shown at higher magnifications. Scale bars = 2.5 μm (a, c), 1.5 μm (b, d). (D) SEM analysis of epicuticular wax crystals on the leaves of transgenic Arabidopsis after induction of *MYB94*. Ten-day-old plants grown in soil were sprayed every 2 d with dimethylsulfoxide (DMSO; mock) or 10 μM β-estradiol solution. Deposition of epicuticular wax crystals was examined 3 weeks after induction. Scale bars = 2 μm.

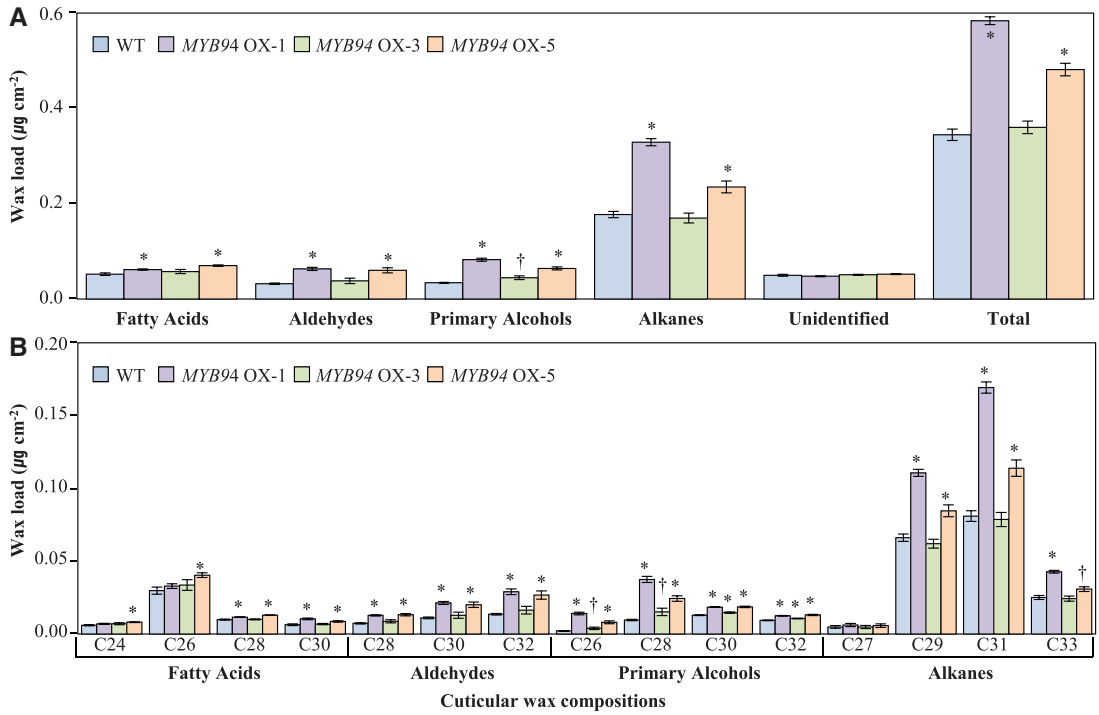

Fig. 4 Cuticular wax composition and amount in the leaves of WT and *MYB94* OX lines. Cuticular waxes were extracted from 3- to 4-week-old leaves (A, B) of Arabidopsis plants. Each value is the mean of five independent measurements. Bars indicate the SE. † and * denote statistical differences with respect to the WT using Student's *t*-test (†$P < 0.05$, *$P < 0.01$).

A

NO.	AGI	FC	P-value	Gene symbol	Target Description
1	At3g47600	16.30	0.0056	*MYB94*	putative transcription factor MYB94
2	At5g37300	16.08	0.0003	*WSD1*	Bifunctional Wax Ester Synthase / Diacylglycerol Acyltransferase
3	At1g04220	3.32	0.0110	*KCS2/DAISY*	Ketoacyl-CoA Synthase
4	At1g02205	2.56	0.0021	*CER1*	CER1-like
5	At4g24510	1.72	0.0003	*CER2*	CER2-like Protein
6	At4g33790	1.65	0.0214	*AlcFAR3 /CER4*	Alcohol-forming Fatty Acyl-CoA Reductase
7	At1g01120	1.62	0.0481	*KCS1*	Ketoacyl-CoA Synthase
8	At3g55360	1.59	0.0027	*ECR/CER10*	Enoyl-CoA Reductase

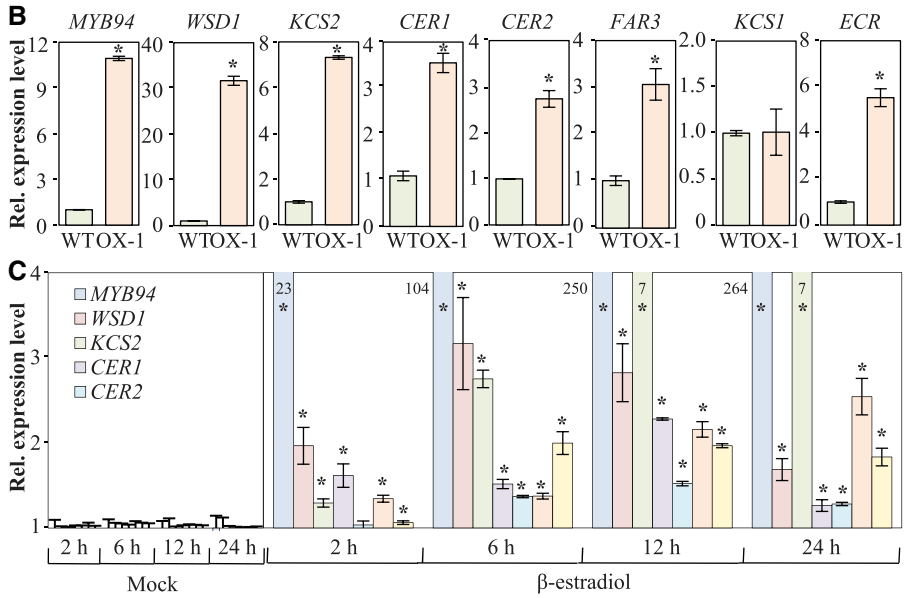

Fig. 5 Up-regulation of cuticular wax biosynthetic genes in *MYB94* OX-1. (A) List of wax biosynthetic genes up-regulated in *MYB94* OX. Genes up-regulated > 1.5-fold in *MYB94* OX compared with the WT are listed. The *P*-values were corrected for multiple testing using FDR (false discovery rate) methodology. AGI, Arabidopsis Genome Initiative number; FC, fold changes. (B, C) qRT–PCR analysis of wax biosynthetic genes. Total RNAs were extracted from the leaves of 3- to 4-week-old WT and *MYB94* OX-1 (B) and from β-estradiol-treated or non-treated leaves of 2-week-old transgenic Arabidopsis (C). Two-week-old transgenic Arabidopsis plants were incubated in MS liquid medium supplemented with DMSO or 10 μM β-estradiol. The total RNA was isolated from whole plants, which were harvested at the indicated time points (hours) after application of DMSO or 10 μM β-estradiol, and were subjected to qRT–PCR analysis. The data from three independent experiments were averaged, and the bars indicate the SE (*t*-test, $*P < 0.05$).

MYB94 activates the expression of wax biosynthetic genes via direct binding of their promoters

To examine if the MYB94 TF regulates the expression of wax biosynthetic genes directly, transcriptional activation assays in tobacco leaf protoplasts and electrophoretic mobility shift assays (EMSAs) were performed. To make reporter constructs, each promoter region of *WSD1*, *KCS2/DAISY*, *CER1*, *CER2*, *FAR3* and *ECR* genes was isolated and transcriptionally fused to the upstream region of the luciferase gene. In addition, the effector constructs with or without a *MYB94* gene under the control of the CaMV 35S promoter were generated (**Fig. 6A**). Then the reporter and effector constructs were co-transformed into tobacco protoplasts, and the luciferase activity was measured. A vector construct harboring the *GUS* gene was included to monitor the transformation efficiencies, and the co-transformation of the p35-*MYB94* effector construct and each reporter construct elevated the luciferase activity by approximately 3.5- to 96-fold (**Fig. 6B**). In contrast, co-transformation with the p35 effector construct and with each reporter construct did not significantly elevate the expression of the reporter gene, indicating that MYB94 functions as a transcriptional activator of the *WSD1*, *KCS2/DAISY*, *CER1*, *CER2*, *FAR3* and *ECR* genes.

We next isolated the MYB binding consensus sequences in the promoter regions of the *WSD1*, *KCS2/DAISY*, *CER1*, *CER2*, *FAR3* and *ECR* genes (as shown in **Supplementary Fig. S4A**; Urao et al. 1993, Abe et al. 2003). The oligonucleotides containing the MYB binding consensus sequences (BS) and their mutant oligonucleotides (mBS) were synthesized and end-labeled with [γ-^{32}P]dATP. The radiolabeled oligonucleotides were incubated with recombinant MYB94:maltose-binding protein (MBP) purified from *Escherichia coli*, and then the reaction mixtures were electrophoresed on 6% native PAGE gels.

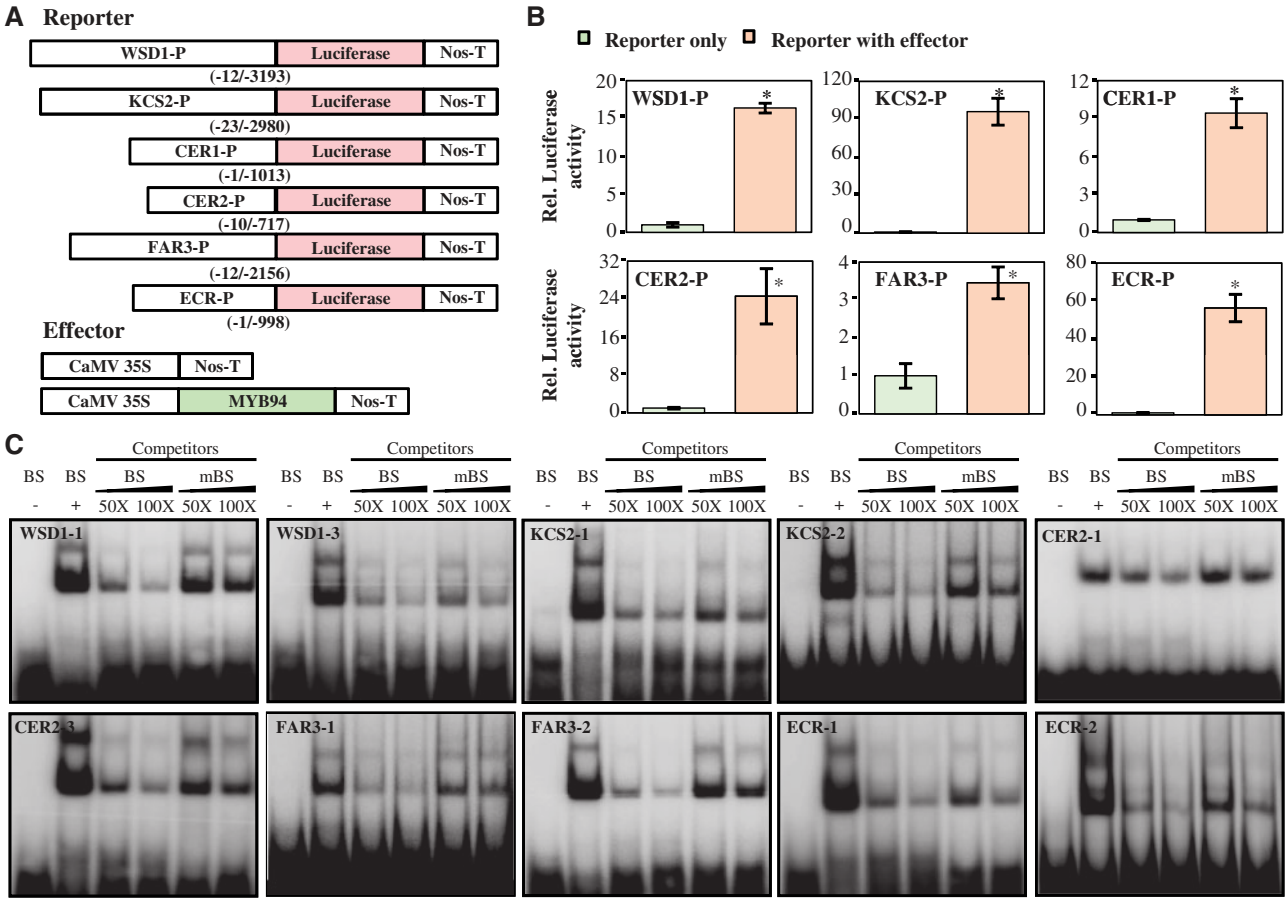

Fig. 6 Binding of MYB94 to consensus motifs in the promoters of wax biosynthetic genes. (A) Schematic diagrams of reporter and effector constructs for the transcriptional activation assay. In the reporter constructs, the promoter regions of the wax biosynthetic genes were fused to the luciferase gene. In the effector construct, MYB94 was cloned between the CaMV 35S promoter and the terminator of the nopaline synthase gene (Nos-T). (B) Transcriptional activation assay in tobacco leaf protoplasts. The reporter and effector constructs shown in (A) were co-transfected into protoplasts, and luciferase activities were determined fluorimetrically. GUS gene expression was used to normalize the luciferase activities, and three measurements were averaged (*t*-test, $*P < 0.05$). The bars indicate the SE. (C) EMSAs. The (−) lanes are controls without recombinant MYB94:MBP proteins, and excess amounts (50× or 100×) of unlabeled BS or mutated BS (mBS) DNA fragments were added as competitors.

As shown in **Fig. 6C**, the MYB94:MBP was bound to the MYB binding consensus motifs of the *WSD1*, *KCS2/DAISY*, *CER2*, *FAR3* and *ECR* gene promoters, but MBP alone did not bind to these. On the other hand, the MYB94:MBP binding was remarkably reduced in the presence of excess amounts of unlabeled BS fragments, and it was reduced to a lesser degree by the mutated BS fragments (mBS), indicating that MYB94 specifically binds to the BS sequences in the *WSD1*, *KCS2/DAISY*, *CER2*, *FAR3* and *ECR* gene promoters. However, no specific binding of the MYB94:MBP to the BSs in the *CER1* promoter was observed (**Supplementary Fig. S4B**). These observations revealed that MYB94 activates the expression of wax biosynthetic genes such as *WSD1*, *KCS2/DAISY*, *CER2*, *FAR3*, and *ECR* via direct binding to their promoters.

Cuticular transpiration occurred more slowly in the leaves of the *MYB94* OX lines compared with those of the WT

To examine if enhanced accumulation of cuticular waxes in *MYB94* OX lines affects water loss through the cuticle, cuticular transpiration assays were carried out. Four-week-old *MYB94* OX and WT plants grown under either normal or drought stress conditions were dark acclimated for 12 h to ensure stomatal closure and were soaked in water for 1 h in the dark. The leaves were then used for water loss measurements. As shown in **Fig. 7**, no significant differences were observed in terms of the cuticular transpiration between *MYB94* OX and WT leaves which were grown under normal conditions. However, cuticular transpiration occurred more slowly in drought-treated *MYB94* OX leaves, but more rapidly in drought-treated WT leaves, indicating that the elevated accumulation of cuticular waxes contributes to a reduction in water loss through the cuticle under water-deficit conditions.

Discussion

The plant surface is covered with a cuticle that is comprised of cutin polyesters and cuticular wax layers. Since the cuticle is the

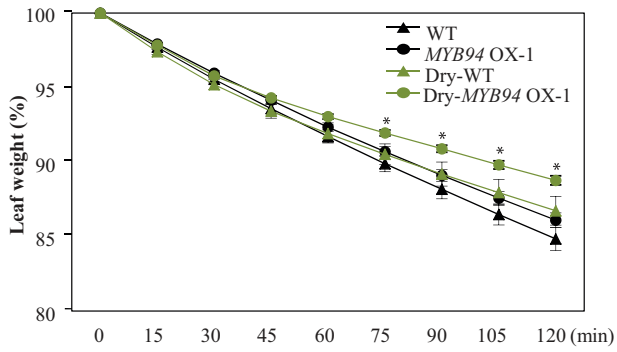

Fig. 7 Cuticular transpiration in WT and *MYB94* OX-1 leaves. Four-week-old plants grown under either normal or drought conditions were acclimated in the dark for 12 h and were soaked in water for 1 h in the dark to equilibrate the water content. The excised rosette leaves were dried and weighed at the indicated time points, and each value is the mean of three independent measurements. The bars indicate the SE, and the asterisks denote statistical differences with respect to the WT (*t*-test, $*P < 0.05$).

first barrier between the plants and their environment, the regulation of cuticle biosynthesis is important for optimal plant growth and for normal plant development. In this study, we identified a novel MYB94 TF that activates Arabidopsis cuticular wax biosynthesis, which is supported by the following evidence: (i) the expression levels of *MYB94* are higher in stem epidermal peels than in stems and are increased significantly by ABA, drought, salt and osmotic stresses; (ii) the MYB94 TF harbors the conserved R2R3 DNA-binding motif at the N-terminus and a transcriptional activation domain at the C-terminus; (iii) MYB94:eYFP was localized in the nucleus in tobacco epidermis and in transgenic Arabidopsis roots; (iv) overexpression of *MYB94* causes the activation of cuticular wax biosynthesis via up-regulation of cuticular wax biosynthetic genes, such as *WSD1*, *KCS2/DAISY*, *CER1*, *CER2*, *FAR3* and *ECR*; and (v) the recombinant MYB94:MBP specifically binds to the MYB consensus motifs in the promoters of the *WSD1*, *KCS2/DAISY*, *CER2*, *FAR3* and *ECR* genes. These findings provide a fundamental insight into the understanding of the regulatory network of cuticular wax biosynthesis and might be useful in the generation of transgenic crops with enhanced tolerance to drought stress.

Several R2R3-type MYB transcriptional activators, including MYB30, MYB41, MYB96, MYB16 and MYB106, have been reported to be involved in cuticular wax biosynthesis or in cuticle development (Cominelli et al. 2008, Raffaele et al. 2008, Seo et al. 2011, Oshima et al. 2013). *MYB94*, as well as *MYB30*, *96*, *16* and *106*, were expressed approximately 8-fold more in stem epidermal peels than in stems (**Supplementary Fig. S1A**; Suh et al. 2005). A particularly strong expression of *MYB94* was observed in the aerial organs of Arabidopsis (**Fig. 2A, C**), and the transcript levels of *MYB94* as well as *MYB96* and *41* were significantly elevated in response to drought stress and ABA treatments (**Fig. 2B**; **Supplementary Fig. S1A**; Cominelli et al. 2008, Seo et al. 2011). Therefore the expression patterns of *MYB94* indicate that *MYB94* might play a role in an increased accumulation of cuticular wax under drought conditions.

It was reported that MYB96 and MYB30 activate VLCFA biosynthesis via up-regulation of genes encoding KCSs and/or KCR1, which are comprised of an FAE complex (Raffaele et al. 2008, Seo et al. 2011). In particular, the contents of most wax components, including aldehydes and alkanes, were remarkably increased in *myb96-1D* relative to the WT, which corresponds to an enhanced synthesis of VLCFAs as precursors for wax biosynthesis (Seo et al. 2011). Similarly, the amount of VLCFAs, primary alcohols and alkanes increased by approximately 35, 140 and 85%, respectively, in *MYB94* OX leaves, as compared with the WT (**Fig. 4**). An increase in the specific wax components is closely associated with an elevated expression of *KCS2/DAISY*, *ECR* and *CER2* genes in VLCFA synthesis (Zheng et al. 2005, Lee et al. 2009b, Haslam et al. 2012), a *CER1* gene in the alkane-forming pathway (Bourdenx et al. 2011) and a *FAR3/CER4* gene in the alcohol-forming pathway (Rowland et al. 2006), which are target genes of a MYB94 TF.

Interestingly, *MYB94* and *MYB96* genes might be generated from a duplication of an ancestral gene (**Supplementary Fig. S1**) and were shown to have a 98% deduced amino acid sequence identity in their DNA-binding domains, but their target genes were found to be distinguishable, except for the *KCS2/DAISY* gene. The target genes of MYB96 were reported to be *KCS1*, *KCS2*, *KCS6* and *KCR1* (Seo et al. 2011), whereas the direct target genes of MYB94 were *WSD1*, *KCS2/DAISY*, *CER2*, *FAR3* and *ECR* (**Fig. 6**), suggesting that each TF independently and/or synergistically contributed to the activation of cuticular wax biosynthesis. According to Lee et al. (2009b), the levels of *KCS2* transcripts were induced by approximately 30- and 65-fold after treatments with ABA and drought, respectively. We found that MYB96 and MYB94 were bound to the same *cis*-element (TAACTACTAACTA) of the *KCS2* promoter by EMSA and/or chromatin immunoprecipitation (ChIP) assay (Seo et al. 2011). Therefore the ABA- or drought-inducible expression of *KCS2* is probably controlled by the synergistic regulation of MYB94 and MYB96. It would be interesting to understand how two different regulatory factors share a *cis*-acting element. It is possible that heterodimers of MYB96 and MYB94 may interact with the *cis*-element of the *KCS2* promoter based on the evidence that two closely related R2R3-MYB proteins, MYB21 and MYB24, form homo- and heterodimers (Song et al. 2011).

In *MYB94* OX leaves compared with the WT, the total amounts of cutin monomers were elevated, but the expression of genes involved in cutin synthesis was not significantly altered (**Supplementary Fig. S3**; **Table S1**). Although there is a possible explanation whereby unidentified genes involved in cutin synthesis are up-regulated by MYB94, the molecular mechanism underlying cutin synthesis in *MYB94* OX plants is still unclear. Kannangara et al. (2007) suggested that the regulation of cutin and wax production by WIN1/SHN1 is a two-step process where the rapid induction of cutin synthesis is followed by the up-regulation of wax biosynthesis. Oshima et al. (2013) observed that MYB106 activates the expression of *WIN1/SHN1* and both MYB106 and WIN1/SHN1 regulate cutin biosynthesis and wax accumulation in a co-ordinated manner.

The levels of *MYB96*, *106* and *WIN1/SHN1* transcripts were observed to have not been significantly altered in *MYB94* OX as compared with the WT, indicating that MYB94 might not be an upstream component of MYB96, MYB106 and WIN1/SHN1. Therefore, the relationship between MYB94 and the other TFs in the regulatory networks of cutin and wax biosynthesis remains to be further investigated.

One interesting point is that an increase in total wax loads was observed in leaves of *MYB94* OX, but not in stems of *MYB94* OX. In previous report, we observed that overexpression of *MYB96* increased total wax loads by approximately 8.6-fold in leaves, but only 1.6-fold in stems (Seo et al. 2011). Kosma et al. (2014) also observed the similar phenotype that overexpression of *MYB41* caused enhanced accumulation of suberin monomers and suberin-associated waxes in leaves, but the amount and composition of suberin monomers were not altered in the roots and seed coats that already contain a lot of suberin monomers. Therefore those results suggest that it might be difficult to observe a higher level of increased cuticular wax loads in stems, where total wax loads are already sufficient.

R2R3-type MYB transcription factors contain the conserved R2R3 domains required for DNA binding at the N-terminus and a highly variable transactivation domain at the C-terminus (Dubos et al. 2010). R2R3 domains are known to bind specifically to the consensus sequence motifs 'YAACKG' and 'CNGTTR' (Urao et al. 1993, Abe et al. 2003). For example, MYB96 directly interacts with MYB consensus motifs that are present in the promoter regions of *KCS1*, *KCS2*, *KCS6*, *KCR1* and *CER3* genes (Seo et al. 2011). The recombinant MYB94:MBP also specifically binds to the MYB consensus motifs in the *WSD1*, *KCS2/DAISY*, *CER2*, *FAR3* and *ECR* promoters (**Fig. 6**; **Supplementary Fig. S4**). In addition, the deletion of the C-terminal region (amino acids 234–323) of MYB30 leads to the inactivation of *pKCS1:GFP:GUS* and *pFDH:GFP:GUS* reporter expression, compared with each reporter and intact MYB30 in the transient assays in *N. benthamiana* leaves (Raffaele et al. 2008), indicating that the transactivation domain of MYB30 is present at the C-terminus of MYB30. Similarly, MYB94 was observed to contain the transactivation domain in its C-terminus (**Fig. 1C**), and we also found that MYB94 harbors the glutamine- and the proline-rich C-terminal region, with characteristics that are frequently associated with transcription activation domains (Tanaka et al. 1994).

TFs were reported to have nuclear localization signals (NLSs) required for their targeting into the nucleus (Boulikas 1994). The fluorescent signals from the MYB94:eYFP construct were observed to be localized in the nucleus in tobacco epidermis and in transgenic Arabidopsis roots (**Fig. 1D**). When the NLS motifs of MYB94 were searched for using a cNLS Mapper (http://nls-mapper.iab.keio.ac.jp/), the region of MYB94 (amino acids 62–92; RPGIKRGNFTEHEEKMILHLQALLGN RWAAI) that overlaps with the DNA-binding domain was detected to be a putative NLS motif. The region is also conserved in other MYB TFs, including MYB16, 30, 41, 96 and 106. In particular, the conserved arginine (R) and lysine (K) residues in the NLSs are probably essential for the import of MYB TFs (Klucevsek et al. 2007, Kosugi et al. 2008).

Cuticle biosynthesis is essential not only for plant growth and development but also for resistance to environmental stress. However, the regulatory mechanisms of cuticle biosynthesis are still largely unknown. In this study, we have identified a novel MYB94 TF that activates cuticular wax biosynthesis via direct transcriptional up-regulation of wax biosynthetic genes. The findings provide fundamental knowledge useful in understanding the molecular mechanisms underlying the regulation of cuticular wax biosynthesis. Considering the results of previous reports where elevated accumulation of cuticular waxes conferred drought tolerance (Aharoni et al. 2004, Zhang et al. 2005, Zhang et al. 2007, Seo et al. 2011), the overexpression of *MYB94*, which did not affect plant growth or development, could be applied to generating drought-tolerant transgenic crops.

Materials and Methods

Plant materials and growth conditions

The seeds of transgenic Arabidopsis (the background is Columbia-0, Col-0) were washed with 70% ethanol for 1 min, 20% bleach for 5 min, and sterilized water. They were then germinated on half-strength Murashige and Skoog (1/2 MS) medium including 1% sucrose and 0.7% phytoagar. The germinated plants were planted on mixed soil (perlite : vermiculite : soil, 1 : 2 : 3) and were grown under long-day conditions (16 h/8 h, light/dark) in a growth room at 24 ± 2°C. Ten-day-old Arabidopsis plants grown in 1/2 MS medium were transferred to MS liquid medium containing 100 μm ABA, 200 mM NaCl or 200 mM mannitol for 1, 2 and 6 h for hormone and stress treatments. To treat drought stress, 2-week-old Arabidopsis plants were air-dried for 1 h and then for 2 h on filter paper.

Construction of binary vectors and Arabidopsis transformation

To generate *MYB94* OX lines, *MYB94* cDNA (1,002 p) was amplified from 2-week-old Arabidopsis plants using the gene-specific primers MYB94_cDNA_F1 (*Sma*I) and MYB94_cDNA_R1 (*Bam*HI), as shown in **Supplementary Table S2**. The amplified products were digested with *Sma*I and *Bam*HI, and were then inserted into the pPZP212 binary vector (Hajdukiewicz et al. 1994). For transient induction of *MYB94* under the control of the β-estradiol-inducible promoter, *MYB94* cDNA was amplified using MYB94_inducible_F1 (*Xho*I) and MYB94_inducible_R1 (*Xho*I). The amplified cDNA was cloned into the same restriction enzyme site of the pER8 vector (Zuo et al. 2000).

The generated constructs were transformed to *Agrobacterium* strain GV3101 using a freeze–thaw method. The transformed *Agrobacterium* cells were then transformed to Arabidopsis plants (Col-0) using vacuum infiltration. The seeds harvested from the transgenic plants were surface sterilized and were germinated on 1/2 MS medium. Each medium includes 25 μg ml^{-1} (w/v) kanamycin and 30 μg ml^{-1} (w/v) hygromycin. The selected transgenic plants (T_2 or T_3 plants) were transferred to mixed soil and were used for further experiments.

Transactivation assay in yeast

The transactivation assay was followed as described in Park et al. (2009). The MYB94-F, MYB94-N and MYB94-C constructs were produced via PCR using *MYB94* cDNA and gene-specific primers (**Supplementary Table S2**). The amplified PCR products were cloned with pGEM T-easy vectors (Promega) and were digested with *Nde*I and *Bam*HI. The digested constructs were cloned with the same restriction enzyme site of the pGBKT7 vector (Clontech). The resultant constructs were transformed to yeast strain Y190 (MATa, HIS3, lacZ, rp1, leu2, cyhr2) and then the transformant was selected from selection medium (SD/−Trp) including 25 mM 3-amino-1,2,4-aminotriazole (3-AT). The selected transformant was cultured in selection medium (SD/−Trp−His) including 25 mM 3-AT for 1 d, and a filter-lift assay was performed for

blue color development in accordance with the method described in Breeden and Nasmyth (1985).

Subcellular localization

To develop the MYB94:eYFP recombinant plasmids, *MYB94* cDNA was amplified using the primers described in **Supplementary Table S2**, digested with *Sma*I restriction enzyme and then cloned into the same restriction enzyme site of the pPZP212 binary vector. The developed construct was transformed to an *Agrobacterium* strain GV3101 and was then injected into the abaxial side of tobacco (*N. benthamiana*) leaf epidermis or transformed to Arabidopsis plants (Col-0). At 36–48 h after injection into tobacco leaves, the eYFP fluorescence was observed under a TCS SP5 AOBS/Tandem laser confocal scanning microscope (Leica). In the case of Arabidopsis, the transgenic seeds were surface sterilized and germinated on the 1/2 MS agar medium including 25 μg ml^{-1} (w/v) kanamycin. Then, the expression of fluorescent protein in the root of 2-week-old transgenic plants (T_2) was observed. The eYFP fluorescence was detected with a YFP filter (excitation, 500 nm; emission, 535 nm). In the case of DAPI staining, the tissues expressing fluorescent protein were stained with DAPI solution [5 μg ml^{-1} in phosphate-buffered saline (PBS)] for 5 min at room temperature, and the signals were observed with a UV filter (excitation, 355 nm; emission, 450 nm) (Yao et al. 2013).

Gene expression analysis

Total RNAs were isolated from various Arabidopsis tissues and from 2-week-old Arabidopsis plants treated with ABA, drought and osmotic stress using an RNeasy® Plant Mini Kit (QIAGEN). Reverse transcription was performed using Gostrip™ Reverse Transcriptase (Promega), and qRT–PCR was performed using SYBR Green I master mix (KAPA) in a 20 μl volume. Gene-specific primers, as described in **Supplementary Table S2**, and a Bio-Rad CFX96 Real-Time PCR system were used for PCR analysis. The *PP2A* (At1g13320) gene was used for normalization.

GUS staining and microscopy

The *MYB94* promoter region (approximately 4.2 kb) was amplified using the MYB94_promoter_F3 and MYB94_promoter_R3 primers and was cloned into the *Hin*dIII and *Sma*I site of the pCAMBIA1391Z binary vector (**Supplementary Table S2**). The produced construct was transformed to the *Agrobacterium* strain GV3101 and transformed to Arabidopsis plants (Col-0). The transgenic plants were selected from 1/2 MS medium including 30 μg ml^{-1} (w/v) hygromycin and were used for histochemical analysis of GUS activation with the method described in Jefferson et al. (1987). The tissues of transgenic plants were stained with GUS staining buffer [100 mM sodium phosphate, pH 7.0, 1 mM 5-bromo-4-chloro-3-indolyl-β-D-glucuronide, 0.5 mM potassium ferrocyanide, 0.5 mM potassium ferricyanide, 10 mM Na_2EDTA and 0.1% (v/v) Triton X-100] overnight at 37°C, and the stained tissues were washed with a series of ethanol solutions ranging from 10% to 100% to remove the Chl. For the leaf cross-sections, stained samples were embedded in Spurr's resin (Ted Pella Inc.) and were then sliced into 20 μm sections using an MT990 microtome (RMC). The images were then observed using a light microscope (L2, Leica).

Scanning electron microscope

A field-emission scanning electron microscope (FE-SEM) was used to examine the epicuticular wax crystals. The third–fourth leaves of WT and *MYB94* OX plants (3–4 weeks old) were cut to 0.5 cm, and were mounted in a 1% osmium tetroxide vapor for 24 h and then air-dried for 1 d. The pieces were mounted onto standard aluminum stubs and were coated with platinum particles using a Hitachi E1030 sputter coater. The surfaces of the coated samples were then observed through a Hitachi S4700 FE-SEM.

Cuticular wax analysis

To analyze the cuticular wax, 0.5 g of 3- to 4-week-old Arabidopsis leaves and 0.1 g of 5-week-old stems were used. Each tissue was dipped in chloroform for 30 s to extract cuticular wax, and then *n*-octacosane, docosanoic acid and 1-tricosanol (Sigma) were added as internal standards. The extracted solution was evaporated under nitrogen gas and was then melted in 100 μl of pyridine and 100 μl of bis-*N*,*N*-(trimethylsilyl)trifluoroacetamide (Sigma). The solution was heat treated at 90°C for 30 min, converted into trimethylsilyl derivatives and was evaporated once more under nitrogen gas. The dried wax complex was dissolved in heptane : toluene (1 : 1), and 1 μl of solution was injected into the gas chromatograph (GC-2010, Shimazu; column 60 m HP-5, 0.32 mm i.d., df = 0.25 mm, Agilent) for quantitative element analysis. The analysis conditions are as follows: injection at 220°C for 4.5 min, an increase of 3°C min^{-1} to 290°C, maintained for 10 min at 290°C, an increase of 2°C min^{-1} to 300°C, and maintained for 15 min at 300°C.

Microarray assays

Affymetrix GeneChip® Arabidopsis Genome ATH1 arrays were carried out to determine the gene expression analysis. The method is as follows: the total RNA was isolated from the leaves of WT and *MYB94* OX-1 (3- to 4-week-old) plants, and the contaminated DNA was removed using RNase-free DNase I (QIAGEN). Synthesis of biotin-labeled cRNA from total RNA, hybridization, detection and scanning were performed according to the manufacturer's procedure. The raw.cel files were used for further analysis. The expression data were generated using Expression Console software (version 1.1). The Affymetrix microarray suite 5 (MAS5) algorithm was used for normalization. To delete the noise during the process of significant gene searching, the probes that did not determine a Present call (>50%) among the MAS5 detection calls were excluded from the analysis. The probe sets that showed a >1.5-fold change compared with the control were selected as differentially regulated genes for the next analysis. The web analysis tool (DAVID, Database for Annotation, Visualization, and Integrated Discovery) was used for biological interpretation analysis of differentially regulated genes, and each functional group was classified by gene function information from the KEGG, Gene ontology database (http://david.abcc.ncifcrf.gov/home.jsp). Three independent assays were performed, and a statistical analysis was performed using the Student's *t*-test. The microarray data were deposited in ArrayExpress with accession number E-MTAB-2870 at https://www.ebi.ac.uk/arrayexpress.

Transcriptional activation assays

The transcriptional activation assays were performed as described in Go et al. (2014). In order to investigate the MYB94 transcriptional activator function, the construct used for development of the overexpression plant (p35S-MYB94) was used as an effector plasmid. The promoter region of the cuticular wax biosynthetic genes was fused with luciferase as a reporter plasmid (**Supplementary Table S2**). The reporter and effector plasmid DNA were co-transfected into tobacco leaf protoplasts and were placed under dark conditions for 16 h. The protoplasts were used for the luciferase activity assay and for the GUS enzymatic assay using a dual-luciferase reporter assay system luminescence reader (GROMAX-20/20: Promega). At this stage, the luciferase gene expression was equalized by the GUS gene expression, showing the relative scores.

Electrophoretic mobility shift assays

The MYB94 N-terminal region (370 bp) was amplified using MYB94-Bam-F and MYB94_yeast_NR1 primer (**Supplementary Table S2**) to perform the EMSAs, and then it was inserted into the *Bam*HI site of the pMAL-c2X *E. coli* expression vector (NEB), including an MBP-coding sequence. The MYB94:MBP protein was extracted using a pMAL™ Protein Fusion and Purification System (#E8000S) method. The synthesized double-stranded oligomers were end-labeled with [γ-^{32}P]dATP using T4 polynucleotide kinase (TAKARA) and were then desalted using chloroform. The extracted recombinant proteins (5 μg) were reacted at room temperature with labeled probes for 30 min in a binding buffer [10 mM Tris–HCl, pH 7.6, 50 mM NaCl, 1 mM Na_2EDTA, 5 mM dithiothreeitol (DTT), 5% glycerol] including 100 ng of poly(dI–dC) under conditions with or without competitors. The reaction mixtures were then electrophoresed by 6% native PAGE, and the gel was dried on paper for scanning in a Typhoon FLA 7000 phosphoimager (GE Healthcare Life Science).

Cuticular transpiration assay

The rate of water loss through the cuticle was estimated using well-watered leaves and drought-treated leaves of 4-week-old plants. Two-week-old plants were subjected to drought stress by withholding water for 2 weeks and were

then rehydrated for 1 d. The rehydrated plants were acclimated in the dark for 12 h and were then soaked in water for 1 h. The weight of the rosette leaves was measured using a micro balance in the dark under a green light (wavelength of approximately 510 nm).

Supplementary data

Supplementary data are available at PCP online.

Funding

This work was supported by the Rural Development Administration, Republic of Korea [grant from the Next-Generation BioGreen 21 Program (No. PJ008203)]; the National Research Foundation of Korea (2013R1A2A 2A01015672)

Acknowledgment

We thank Juyoung Kim at Chonnam National University for technical assistance in yeast transactivation assay and subcellular localization analysis.

Disclosures

The authors have no conflicts of interest to declare.

References

Abe, H., Urao, T., Ito, T., Seki, M., Shinozaki, K. and Yamaguchi-Shinozaki, K. (2003) Arabidopsis AtMYC2 (bHLH) and AtMYB2 (MYB) function as transcriptional activators in abscisic acid signaling. *Plant Cell* 15: 63–78.

Aharoni, A., Dixit, S., Jetter, R., Thoenes, E., van Arkel, G. and Pereira, A. (2004) The SHINE clade of AP2 domain transcription factors activates wax biosynthesis, alters cuticle properties, and confers drought tolerance when overexpressed in Arabidopsis. *Plant Cell* 16: 2463–2480.

Beisson, F., Li-Beisson, Y. and Pollard, M. (2012) Solving the puzzles of cutin and suberin polymer biosynthesis. *Curr. Opin. Plant Biol.* 15: 329–337.

Bernard, A., Domergue, F., Pascal, S., Jetter, R., Renne, C., Faure, J.D. et al. (2012) Reconstitution of plant alkane biosynthesis in yeast demonstrates that Arabidopsis ECERIFERUM1 and ECERIFERUM3 are core components of a very-long-chain alkane synthesis complex. *Plant Cell* 24: 3106–3118.

Bernard, A. and Joubes, J. (2013) Arabidopsis cuticular waxes: advances in synthesis, export and regulation. *Prog. Lipid Res.* 52: 110–129.

Boulikas, T. (1994) Putative nuclear localization signals (NLS) in protein transcription factors. *J. Cell Biochem.* 55: 32–58.

Bourdenx, B., Bernard, A., Domergue, F., Pascal, S., Leger, A., Roby, D. et al. (2011) Overexpression of Arabidopsis ECERIFERUM1 promotes wax very-long-chain alkane biosynthesis and influences plant response to biotic and abiotic stresses. *Plant Physiol.* 156: 29–45.

Breeden, L. and Nasmyth, K. (1985) Regulation of the yeast HO gene. *Cold Spring Harb. Symp. Quant. Biol.* 50: 643–650.

Broun, P., Poindexter, P., Osborne, E., Jiang, C.Z. and Riechmann, J.L. (2004) WIN1, a transcriptional activator of epidermal wax accumulation in Arabidopsis. *Proc. Natl Acad. Sci. USA* 101: 4706–4711.

Cameron, K.D., Teece, M.A. and Smart, L.B. (2006) Increased accumulation of cuticular wax and expression of lipid transfer protein in response to periodic drying events in leaves of tree tobacco. *Plant Physiol.* 140: 176–183.

Cominelli, E., Sala, T., Calvi, D., Gusmaroli, G. and Tonelli, C. (2008) Overexpression of the Arabidopsis AtMYB41 gene alters cell expansion and leaf surface permeability. *Plant J.* 53: 53–64.

Debono, A., Yeats, T.H., Rose, J.K., Bird, D., Jetter, R., Kunst, L. et al. (2009) Arabidopsis LTPG is a glycosylphosphatidylinositol-anchored lipid transfer protein required for export of lipids to the plant surface. *Plant Cell* 21: 1230–1238.

Dubos, C., Stracke, R., Grotewold, E., Weisshaar, B., Martin, C. and Lepiniec, L. (2010) MYB transcription factors in Arabidopsis. *Trends Plant Sci.* 15: 573–581.

Go, Y.S., Kim, H., Kim, H.J. and Suh, M.C. (2014) Arabidopsis cuticular wax biosynthesis is negatively regulated by the DEWAX gene encoding an AP2/ERF-type transcription factor. *Plant Cell* 26: 1666–1680.

Greer, S., Wen, M., Bird, D., Wu, X.M., Samuels, L., Kunst, L. et al. (2007) The cytochrome P450 enzyme CYP96A15 is the midchain alkane hydroxylase responsible for formation of secondary alcohols and ketones in stem cuticular wax of Arabidopsis. *Plant Physiol.* 145: 653–667.

Hajdukiewicz, P., Svab, Z. and Maliga, P. (1994) The small, versatile pPZP family of Agrobacterium binary vectors for plant transformation. *Plant Mol. Biol.* 25: 989–994.

Haslam, T.M., Manas-Fernandez, A., Zhao, L. and Kunst, L. (2012) Arabidopsis ECERIFERUM2 is a component of the fatty acid elongation machinery required for fatty acid extension to exceptional lengths. *Plant Physiol.* 160: 1164–1174.

Jefferson, R.A., Kavanagh, T.A. and Bevan, M.W. (1987) GUS fusions: β-glucuronidase as a sensitive and versatile gene fusion marker in higher plants. *EMBO J.* 6: 3901–3907.

Jetter, R., Kunst, L. and Samuels, A.L. (2006) Composition of plant cuticular waxes. *In* Biology of the Plant Cuticle. Edited by Riederer, M. and Müller, C. pp. 145–181. Blackwell Publishing, Oxford.

Kannangara, R., Branigan, C., Liu, Y., Penfield, T., Rao, V., Mouille, G. et al. (2007) The transcription factor WIN1/SHN1 regulates cutin biosynthesis in Arabidopsis thaliana. *Plant Cell* 19: 1278–1294.

Kim, H., Lee, S.B., Kim, H.J., Min, M.K., Hwang, I. and Suh, M.C. (2012) Characterization of glycosylphosphatidylinositol-anchored lipid transfer protein 2 (LTPG2) and overlapping function between LTPG/LTPG1 and LTPG2 in cuticular wax export or accumulation in Arabidopsis thaliana. *Plant Cell Physiol.* 53: 1391–1403.

Klucevsek, K., Wertz, M., Lucchi, J., Leszczynski, A. and Moroianu, J. (2007) Characterization of the nuclear localization signal of high risk HPV16 E2 protein. *Virology* 360: 191–198.

Kosma, D.K., Bourdenx, B., Bernard, A., Parsons, E.P., Lu, S., Joubes, J. et al. (2009) The impact of water deficiency on leaf cuticle lipids of Arabidopsis. *Plant Physiol.* 151: 1918–1929.

Kosma, D.K., Murmu, J., Razeq, F.M., Santos, P., Bourgault, R., Molina, I. et al. (2014) AtMYB41 activates ectopic suberin synthesis and assembly in multiple plant species and cell types. *Plant J.* 80: 216–229.

Kosugi, S., Hasebe, M., Entani, T., Takayama, S., Tomita, M. and Yanagawa, H. (2008) Design of peptide inhibitors for the importin αβ nuclear import pathway by activity-based profiling. *Chem. Biol.* 15: 940–949.

Kunst, L. and Samuels, L. (2009) Plant cuticles shine: advances in wax biosynthesis and export. *Curr. Opin. Plant Biol.* 12: 721–727.

Lee, S.B., Go, Y.S., Bae, H.J., Park, J.H., Cho, S.H., Cho, H.J. et al. (2009a) Disruption of glycosylphosphatidylinositol-anchored lipid transfer protein gene altered cuticular lipid composition, increased plastoglobules, and enhanced susceptibility to infection by the fungal pathogen Alternaria brassicicola. *Plant Physiol.* 150: 42–54.

Lee, S.B., Jung, S.J., Go, Y.S., Kim, H.U., Kim, J.K., Cho, H.J. et al. (2009b) Two Arabidopsis 3-ketoacyl CoA synthase genes, KCS20 and KCS2/DAISY, are functionally redundant in cuticular wax and root suberin biosynthesis, but differentially controlled by osmotic stress. *Plant J.* 60: 462–475.

Lee, S.B. and Suh, M.C. (2013) Recent advances in cuticular wax biosynthesis and its regulation in Arabidopsis. *Mol. Plant* 6: 246–249.

Li-Beisson, Y., Shorrosh, B., Beisson, F., Andersson, M.X., Arondel, V., Bates, P.D. et al. (2013) Acyl-lipid metabolism. *Arabidopsis Book* 11: e0161.

Li, F., Wu, X., Lam, P., Bird, D., Zheng, H., Samuels, L. et al. (2008) Identification of the wax ester synthase/acyl-coenzyme A: diacylglycerol acyltransferase WSD1 required for stem wax ester biosynthesis in Arabidopsis. *Plant Physiol.* 148: 97–107.

Liu, Q., Kasuga, M., Sakuma, Y., Abe, H., Miura, S., Yamaguchi-Shinozaki, K. et al. (1998) Two transcription factors, DREB1 and DREB2, with an EREBP/AP2 DNA binding domain separate two cellular signal transduction pathways in drought-and low-temperature-responsive gene expression, respectively, in Arabidopsis. *Plant Cell* 10: 1391–1406.

Lu, S., Song, T., Kosma, D.K., Parsons, E.P., Rowland, O. and Jenks, M.A. (2009) Arabidopsis CER8 encodes long-chain acyl CoA synthetase 1 (LACS1) that has overlapping functions with LACS2 in plant wax and cutin synthesis. *Plant J.* 59: 553–564.

McFarlane, H.E., Shin, J.H., Bird, D.A. and Samuels, A.L. (2010) Arabidopsis ABCG transporters, which are required for export of diverse cuticular lipids, dimerize in different combinations. *Plant Cell* 22: 3066–3075.

McFarlane, H.E., Watanabe, Y., Yang, W., Huang, Y., Ohlrogge, J. and Samuels, A.L. (2014) Golgi- and trans-Golgi network-mediated vesicle trafficking is required for wax secretion from epidermal cells. *Plant Physiol.* 164: 1250–1260.

Oshima, Y., Shikata, M., Koyama, T., Ohtsubo, N., Mitsuda, N. and Ohme-Takagi, M. (2013) MIXTA-like transcription factors and WAX INDUCER1/SHINE1 coordinately regulate cuticle development in Arabidopsis and Torenia fournieri. *Plant Cell* 25: 1609–1624.

Pascal, S., Bernard, A., Sorel, M., Pervent, M., Vile, D., Haslam, R.P. et al. (2013) The Arabidopsis cer26 mutant, like the cer2 mutant, is specifically affected in the very-long-chain fatty acid elongation process. *Plant J.* 73: 733–746.

Park, J., Kim, M.J., Jung, S.J. and Suh, M.C. (2009) Identification of a novel transcription factor, AtBSD1, containing a BSD domain in Arabidopsis thaliana. *J. Plant Biol.* 52: 141–146.

Raffaele, S., Vailleau, F., Leger, A., Joubes, J., Miersch, O., Huard, C. et al. (2008) A MYB transcription factor regulates very-long-chain fatty acid biosynthesis for activation of the hypersensitive cell death response in Arabidopsis. *Plant Cell* 20: 752–767.

Rowland, O., Zheng, H., Hepworth, S.R., Lam, P., Jetter, R. and Kunst, L. (2006) CER4 encodes an alcohol-forming fatty acyl-coenzyme A reductase involved in cuticular wax production in Arabidopsis. *Plant Physiol.* 142: 866–877.

Seo, P.J., Lee, S.B., Suh, M.C., Park, M.J., Go, Y.S. and Park, C.M. (2011) The MYB96 transcription factor regulates cuticular wax biosynthesis under drought conditions in Arabidopsis. *Plant Cell* 23: 1138–1152.

Shephered, T. and Griffiths, D.W. (2006) The effects of stress on plant cuticular waxes. *New Phytol.* 171: 469–499.

Song, S., Qi, T., Huang, H., Ren, Q., Wu, D., Chang, C. et al. (2011) The Jasmonate-ZIM domain proteins interact with the R2R3-MYB transcription factors MYB21 and MYB24 to affect Jasmonate-regulated stamen development in Arabidopsis. *Plant Cell* 23: 1000–1013.

Sparkes, I.A., Runions, J., Kearns, A. and Hawes, C. (2006) Rapid, transient expression of fluorescent fusion proteins in tobacco plants and generation of stably transformed plants. *Nat. Protoc.* 1: 2019–2025.

Suh, M.C., Samuels, A.L., Jetter, R., Kunst, L., Pollard, M., Ohlrogge, J. et al. (2005) Cuticular lipid composition, surface structure, and gene expression in Arabidopsis stem epidermis. *Plant Physiol.* 139: 1649–1665.

Tanaka, M., Clouston, W.M. and Herr, W. (1994) The Oct-2 glutamine-rich and proline-rich activation domains can synergize with each other or duplicates of themselves to activate transcription. *Mol. Cell. Biol.* 14: 6046–6055.

Urao, T., Yamaguchi-Shinozaki, K., Urao, S. and Shinozaki, K. (1993) An Arabidopsis myb homolog is induced by dehydration stress and its gene product binds to the conserved MYB recognition sequence. *Plant Cell* 5: 1529–1539.

Weng, H., Moilina, I., Shockey, J. and Browse, J. (2010) Organ fusion and defective cuticle function in a *lacs1 lacs2* double mutant. *Planta* 231: 1089–1100.

Winter, D., Vinegar, B., Nahal, H., Ammar, R., Wilson, G.V. and Provart, N.J. (2007) An 'Electronic Fluorescent Pictograph' browser for exploring and analyzing large-scale biological data sets. *PloS one* 2: e718.

Wu, R., Li, S., He, S., Wassmann, F., Yu, C., Qin, G. et al. (2011) CFL1, a WW domain protein, regulates cuticle development by modulating the function of HDG1, a class IV homeodomain transcription factor, in rice and Arabidopsis. *Plant Cell* 23: 3392–3411.

Yao, H., Wang, G., Guo, L. and Wang, X. (2013) Phosphatidic acid interacts with a MYB transcription factor and regulates its nuclear localization and function in Arabidopsis. *Plant Cell* 25: 5030–5042.

Yeats, T.H. and Rose, J.K.C. (2013) The formation and function of plant cuticles. *Plant Physiol.* 163: 5–29.

Zhang, J.Y., Broeckling, C.D., Blancaflor, E.B., Sledge, M.K., Sumner, L.W. and Wang, Z.Y. (2005) Overexpression of WXP1, a putative Medicago truncatula AP2 domain-containing transcription factor gene, increases cuticular wax accumulation and enhances drought tolerance in transgenic alfalfa (Medicago sativa). *Plant J.* 42: 689–707.

Zhang, J.Y., Broeckling, C.D., Sumner, L.W. and Wang, Z.Y. (2007) Heterologous expression of two Medicago truncatula putative ERF transcription factor genes, WXP1 and WXP2, in Arabidopsis led to increased leaf wax accumulation and improved drought tolerance, but differential response in freezing tolerance. *Plant Mol. Biol.* 64: 265–278.

Zhang, X., Henriques, R., Lin, S.-S., Niu, Q.-W. and Chua, N.-H. (2006) Agrobacterium-mediated transformation of Arabidopsis thaliana using the floral dip method. *Nat. Protoc.* 1: 641–646.

Zheng, H., Rowland, O. and Kunst, L. (2005) Disruptions of the Arabidopsis enoyl-CoA reductase gene reveal an essential role for very-long-chain fatty acid synthesis in cell expansion during plant morphogenesis. *Plant Cell* 17: 1467–1481.

Zuo, J., Niu, Q.W. and Chua, N.H. (2000) An estrogen receptor-based transactivator XVE mediates highly inducible gene expression in transgenic plants. *Plant J.* 24: 265–273.